

Short Communication

## The Effect of Calcination Time on the Electrochemical Performance of Doped $\text{LiMg}_{0.02}\text{Mn}_{1.98}\text{O}_4$ cathode Material Prepared by Solid-State Combustion Synthesis

Mingwu Xiang<sup>1,2</sup>, Bin Li<sup>1,2</sup>, Zhifang Zhang<sup>1,2</sup>, Cancan Peng<sup>1,2</sup>, Hongli Bai<sup>1,2</sup>, Changwei Su<sup>1,2</sup>, Junming Guo<sup>1,2, \*</sup>

<sup>1</sup> Engineering Research Center of Biopolymer Functional Materials of Yunnan, Yunnan University of Nationalities, Kunming 650500, P. R. China

<sup>2</sup> Key Laboratory of Chemistry in Ethnic Medicinal Resources, State Ethnic Affairs Commission & Ministry of Education, Yunnan University of Nationalities, Kunming 650500, P. R. China

\*E-mail: [guojunming@tsinghua.org.cn](mailto:guojunming@tsinghua.org.cn)

Received: 11 October 2013 / Accepted: 19 November 2013 / Published: 8 December 2013

$\text{LiMg}_{0.02}\text{Mn}_{1.98}\text{O}_4$  cathode materials were synthesized by a solid-state combustion synthesis process at 500°C for various calcining time. The morphology and crystal structure of the samples were characterized by scanning electron microscopy (SEM) and X-ray diffraction (XRD). All samples had single phase spinel  $\text{LiMn}_2\text{O}_4$  structure, and its crystallinity and particulate sizes increase with the increase of calcination time. The electrochemical performance of the samples were investigated by charge-discharge cycling test and cyclic voltammetry. The cycling stability of  $\text{LiMg}_{0.02}\text{Mn}_{1.98}\text{O}_4$  was improved attribute to the Mg-doping.  $\text{LiMg}_{0.02}\text{Mn}_{1.98}\text{O}_4$  synthesized at calcination time of 6 h had excellent electrochemical performance with an initial specific discharge capacity of 107.2 mAh g<sup>-1</sup> at 0.2 C and a capacity retention of 88.62% after 100 cycles.

**Keywords:** Solid-state combustion synthesis;  $\text{LiMn}_2\text{O}_4$ ; Lithium ion battery; cathode material

### 1. INTRODUCTION

As is known to all, rechargeable lithium-ion batteries (LIBs) are widely applied to portable systems, such as telephones, computers, telecommunication devices, hybrid electric vehicles (HEVs) and full electric vehicles (EVs) [1, 2]. Recently, there exist three types of structural materials including  $\text{LiCoO}_2$  in a layer structure,  $\text{LiFePO}_4$  in an olivine structure and  $\text{LiMn}_2\text{O}_4$  in a spinel structure that are used as cathode materials for (LIBs) [3]. While spinel  $\text{LiMn}_2\text{O}_4$  has been extensively studied as the most promising cathode materials for (LIBs) due to its abundant resources, low cost, good safety and environmental friendliness [3, 4]. Spinel  $\text{LiMn}_2\text{O}_4$  materials had been prepared by many synthetic

techniques, for instance, solid-state process [5-7], molten salts synthesis [8, 9], sol-gel method [10, 11] and hydrothermal synthesis [12]. In our previous work,  $\text{LiMn}_2\text{O}_4$  cathode materials were synthesized successfully by the solid-state combustion synthesis method, which is firstly proposed by our team [13]. And the influence of organic fuel and calcination temperature on electrochemical performance of  $\text{LiMn}_2\text{O}_4$  materials had been investigated [14]. Compared with other methods, solid-state combustion synthesis possesses these advantages of quick reaction rate, required low reaction temperature and simplical process.

In this work,  $\text{LiMg}_{0.02}\text{Mn}_{1.98}\text{O}_4$  cathode materials were prepared by solid-state combustion synthesis calcined at  $500^\circ\text{C}$  for different time with manganese carbonate and lithium carbonate as raw materials, magnesium acetate as  $\text{Mg}^{2+}$  dopant and citric acid as a fuel. The electrochemical performance of syntheticed materials was improved by Mg-doping, and the influence of calcination time on the crystal structure, morphology and electrochemical properties of  $\text{LiMg}_{0.02}\text{Mn}_{1.98}\text{O}_4$  were investigated.

## 2. EXPERIMENTAL

### 2.1. Preparation of $\text{LiMg}_{0.02}\text{Mn}_{1.98}\text{O}_4$ Materials

$\text{LiMg}_{0.02}\text{Mn}_{1.98}\text{O}_4$  products were prepared by a solid-state combustion synthesis. Firstly, lithium carbonate (AR, Sinopharm Chemical reagent Co., Ltd.), manganese carbonate (AR, alading) and magnesium acetate (AR, Sinopharm Chemical reagent Co., Ltd.) were weighted and put into a 500 mL polytetrafluoroethylene jar (the stoichiometric amounts of Li:Mn:Mg = 1:1.98:0.02, a total mixture mass of 30.0 g). A given amount 5wt% of gross weight of citric acid (AR, Sinopharm Chemical reagent Co., Ltd.) was added into the mixture and then ball-milled thoroughly by planetary ball mill with ethanol as medium. The reaction mixture was off-white powder after drying. Subsequently, 5.5 g of the reaction mixture was placed in an alumina crucible and then calcined in muffle furnace at  $500^\circ\text{C}$  for 1, 3, 6 and 9 h in air atmosphere, respectively. The black  $\text{LiMg}_{0.02}\text{Mn}_{1.98}\text{O}_4$  powders were obtained after naturally cooling to ambient temperature.

### 2.2. Characterization of $\text{LiMg}_{0.02}\text{Mn}_{1.98}\text{O}_4$ Materials

Characterization of  $\text{LiMg}_{0.02}\text{Mn}_{1.98}\text{O}_4$  powders was carried out by X-ray diffraction (XRD, D/max-TTRIII, Japan) with  $\text{CuK}\alpha$  radiation to identify the crystal structure and the measurement range was from  $10^\circ$  to  $70^\circ$  with  $0.02^\circ$  step size and scan speed was  $4^\circ \text{min}^{-1}$  at an operation current of 30 mA and voltage of 40 kV. The microstructure morphology of the  $\text{LiMg}_{0.02}\text{Mn}_{1.98}\text{O}_4$  powder was observed by scanning electron microscopy (SEM, QUANTA-200 America FEI Company).

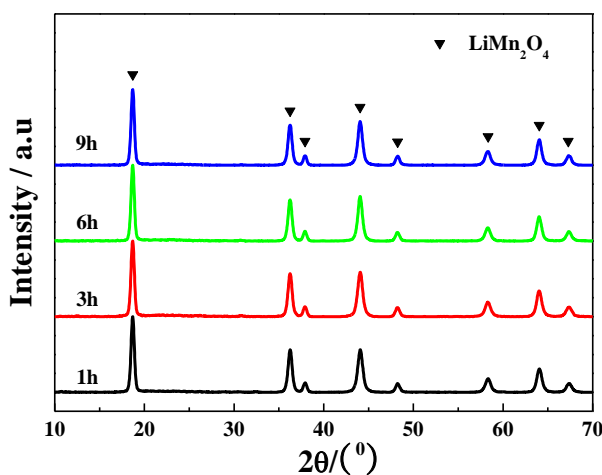
### 2.3. Electrochemical Studies of $\text{LiMg}_{0.02}\text{Mn}_{1.98}\text{O}_4$ Materials

For electrochemical measurements, the cathode electrodes were fabricated by mixing the  $\text{LiMg}_{0.02}\text{Mn}_{1.98}\text{O}_4$  powders, polyvinylidene fluoride (PVDF) and acetylene black with a mass ratio of

8:1:1 in a 100 mL jar mill filled with appropriate N-methyl-2-pyrrolidone (NMP) solvent for the binder. The slurry mixture was formed after fully ball-mill mixing and then spread uniformly on an aluminum foil by using doctor-blade technique. The paste film after drying in an oven at 80°C for 4 h was punched into circular disk with 16 mm diameter after pressure rolling. All prepared cathode disks were dried at 120°C in vacuum oven for overnight before cell assembling. Using Celgard 2320-type membrane as the separator, lithium metal foil as the counter electrode, 1 M LiPF<sub>6</sub> in ethylene carbonate (EC)-1,2-dimethyl carbonate (DMC) as the electrolyte (EC and DMC volume ratio of 1:1), CR2025 coin-type cell was assembled in a dry glove box filled with high purity argon gas. Galvanostatical charge-discharge experiments were performed by Land electric test system CT2001A (Wuhan Jinnuo Electronics Co., Ltd.) at a current density of 0.2 C between 3.20 and 4.35V ( versus Li/Li<sup>+</sup> ). Cyclic voltammogram (CV) tests were carried out on ZAHNER Zennium IM6 Electrochemical Workstation (ZAHNER-elektrik GmbH & Co. KG, Kronach, Germany) at a scan rate of 0.05 mV s<sup>-1</sup>. The LiMg<sub>0.02</sub>Mn<sub>1.98</sub>O<sub>4</sub> was used as cathode material and metallic lithium as the counter and reference anode. All the electrochemical measurements were carried out at ambient temperature.

### 3. RESULTS AND DISCUSSION

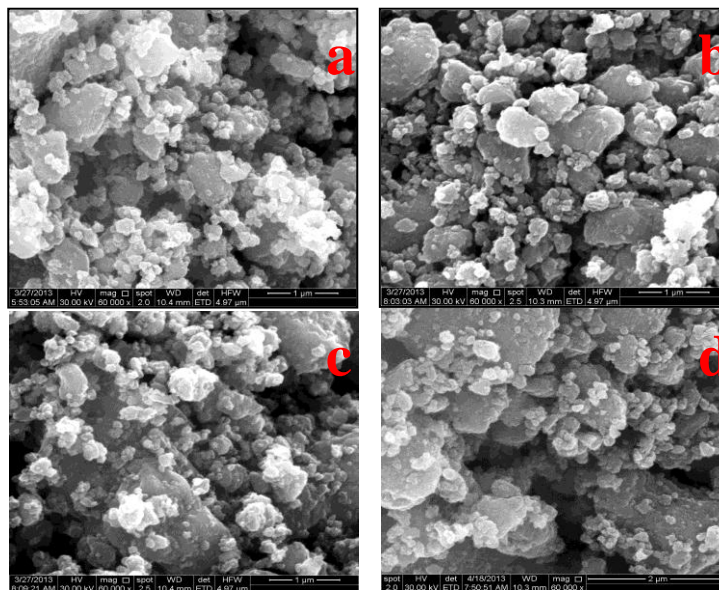
#### 3.1. Analysis of Structure and Morphology



**Figure 1.** XRD patterns of LiMg<sub>0.02</sub>Mn<sub>1.98</sub>O<sub>4</sub> samples

Fig. 1 shows the XRD patterns of LiMg<sub>0.02</sub>Mn<sub>1.98</sub>O<sub>4</sub> as-prepared at 500°C for various time. The characteristic peaks of the spinel LiMn<sub>2</sub>O<sub>4</sub> (JCPDS, PDF 35-0782) [15], for example, the (1 1 1), (3 1 1), (2 2 2), (4 0 0), (3 3 1), (5 1 1), (4 4 0) and (5 3 1) peaks are detected in Fig. 1. All synthetic products are single phase and no impurities such as manganese or magnesium oxide compounds are detected, which indicates the main spinel crystal structure of LiMn<sub>2</sub>O<sub>4</sub> was not changed after doping Mg and calcining for various time. The crystallinity of LiMg<sub>0.02</sub>Mn<sub>1.98</sub>O<sub>4</sub> gradually increases with the increase of calcination time. In particular, LiMg<sub>0.02</sub>Mn<sub>1.98</sub>O<sub>4</sub> calcined for 6 h has a minimum full width at half maximum (FWHM), implying that it has a well-crystallized and an ordered spinel structure with

a space group of  $Fd3m$  [16]. The XRD results demonstrate that the solid-state combustion synthesis in the present work can synthesize single-phased  $\text{LiMn}_2\text{O}_4$  products.



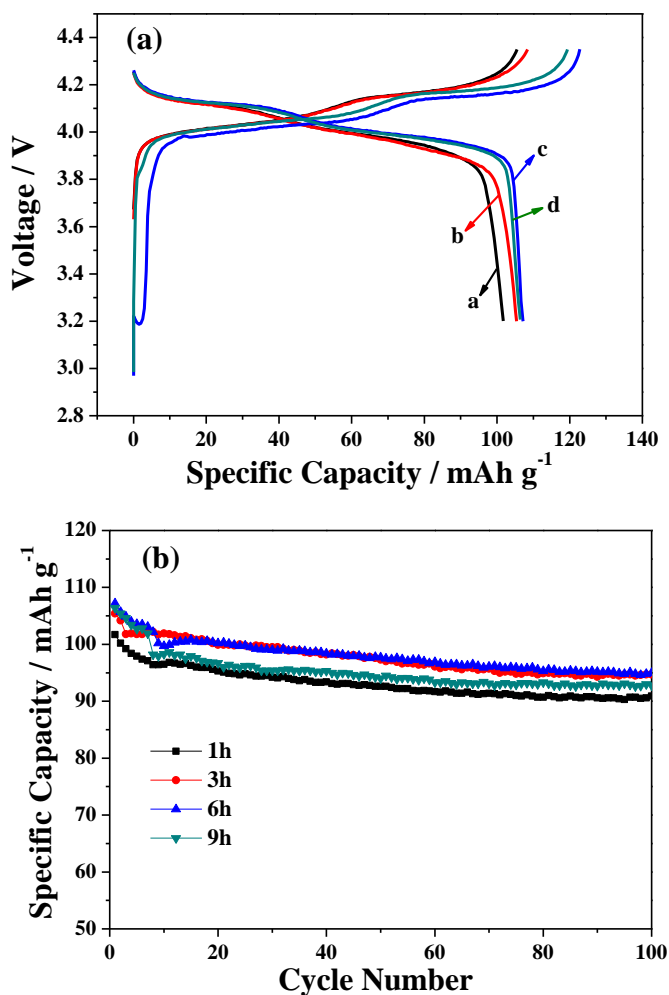
**Figure 2.** SEM images of  $\text{LiMg}_{0.02}\text{Mn}_{1.98}\text{O}_4$  samples following calcination time for a: 1 h, b: 3 h, c: 6 h and d: 9 h

Fig. 2 shows the SEM images of  $\text{LiMg}_{0.02}\text{Mn}_{1.98}\text{O}_4$  calcined at  $500^\circ\text{C}$  for different time. It can be observed that the morphologies of all products were agglomerated and it consists of complex crystalline grains of sizes in the range  $0.1 - 0.3 \mu\text{m}$ , which are composed of much smaller crystallites. There are many scattered grains in small sizes stick on the surface of these larger particles. The grain grow more completely, particle agglomerate seriously and maldistribution with the increase of the calcination time.

### 3.2. Galvanostatic Cycling

Fig. 3 shows the first galvanostatic charge–discharge profiles (a) and cycling performance curves (b) of  $\text{LiMg}_{0.02}\text{Mn}_{1.98}\text{O}_4$  products at  $0.2 \text{ C}$  rate and in the voltage range of  $3.20\sim 4.35 \text{ V}$ . Two potential plateaus at around  $3.90$  and  $4.20 \text{ V}$  were observed for all products, which corresponds to that of the two-stage intercalation/de-intercalation process of lithium in spinel  $\text{LiMn}_2\text{O}_4$  [17], indicating that Mg-doping or different calcination time didn't change the electrochemical reaction of lithium-ion during charge/discharge process. As shown in Fig. 3(b) and table 1, the initial discharge specific capacity and capacity retention tend to reduce after the increase with the increase of calcination time. The Mg-doped  $\text{LiMg}_{0.02}\text{Mn}_{1.98}\text{O}_4$  products have higher capacity retention than that of pristine  $\text{LiMn}_2\text{O}_4$  [13] (the capacity retention of  $85.00\%$  with the same voltage at  $0.2\text{C}$  cycling 40 times), suggesting that Mg-doping significantly improved the capacity retention of  $\text{LiMn}_2\text{O}_4$ . Because the structural stability of spinel  $\text{LiMn}_2\text{O}_4$  was strengthened due to  $\text{Mg}^{2+}$  ions partially substituted for  $\text{Mn}^{3+}$

ion in the octahedral 16d sites, results in the initial discharge specific capacity was reduced and capacity retention was improved.



**Figure 3.** First galvanostatic charge-discharge curves (a) (a: 1 h, b: 3 h, c: 6 h and d: 9 h), Cycling performance curves (b) of  $\text{LiMg}_{0.02}\text{Mn}_{1.98}\text{O}_4$  samples between 3.20 and 4.35 V at 0.2 C rate.

**Table 1.** Discharge specific capacity and capacity retention of  $\text{LiMg}_{0.02}\text{Mn}_{1.98}\text{O}_4$  samples.

Time (h)	Discharge specific capacity ( $\text{mAh g}^{-1}$ )		Capacity retentions (%)
	First cycle	100th cycle	
1	101.7	90.90	89.38
3	105.4	94.70	89.85
6	107.2	95.00	88.62
9	106.4	92.80	87.22

This results was in good agreement with reported literatures [18-20]. Particularly,  $\text{LiMg}_{0.02}\text{Mn}_{1.98}\text{O}_4$  synthesized for calcination time of 6 h reveals the excellent electrochemical

performance with an initial specific discharge capacity of  $107.2 \text{ mAh g}^{-1}$  at  $0.2 \text{ C}$  and a capacity retention of  $88.62\%$  after 100 cycles.

### 3.3. Cyclic Voltammetry

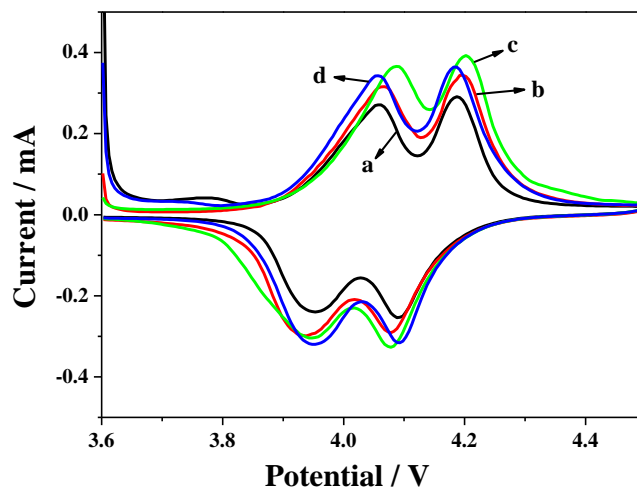


**Figure 4.** Cyclic voltammogram curves of the  $\text{LiMg}_{0.02}\text{Mn}_{1.98}\text{O}_4$  samples following calcination time (a: 1 h, b: 3 h, c: 6 h, and d: 9 h)

In order to study the electrochemical cycling reversibility of synthetic materials. The cyclic voltammograms of  $\text{LiMg}_{0.02}\text{Mn}_{1.98}\text{O}_4$  electrodes prepared at different calcination time are shown in Fig. 4. The cells are cycled in the potential range  $3.60\text{--}4.50\text{V}$  (vs.  $\text{Li}/\text{Li}^+/\text{V}$ ) and at a scan rate of  $0.05 \text{ mV s}^{-1}$ . The two pairs of well separated redox peaks (at  $4.08 \text{ V}/3.95 \text{ V}$  and  $4.20 \text{ V}/4.09 \text{ V}$ ) for all materials were obviously observed from Fig. 4, which are commendably consistent with the two potential plateaus in the charge-discharge curves following Fig. 3.(a), suggesting that lithium-ion are extracted and inserted from/into the spinel phase by a two-step process [21, 22]. Further indicating Mg-substitution does not affect severely the redox potentials of  $\text{LiMn}_2\text{O}_4$  [23]. The two pairs of redox peaks for all synthetic materials are well-defined splitting and symmetric, suggesting that the intercalation/ de-intercalation of lithium-ion into/from the spinel phase were reversible. Both the anodic and cathodic peak currents of synthetic  $\text{LiMg}_{0.02}\text{Mn}_{1.98}\text{O}_4$  materials increase with the extension of calcination time from 1 h to 6 h, while, that of sample prepared by calcination of 9 h decreasing slightly. The phenomenon may be explained as following: 1) The increase of peak currents suggested the electrochemical activity and specific capacity were improved due to the crystallinity of the  $\text{LiMg}_{0.02}\text{Mn}_{1.98}\text{O}_4$  materials increased with the increase of calcination time from 1 h to 6 h [24]. 2) The particle growth of the  $\text{LiMg}_{0.02}\text{Mn}_{1.98}\text{O}_4$  material prepared by a too long time calcination was a little larger, which reduced the  $\text{Li}^+$  ion diffusion rate in the charge/discharge process, resulting in slightly decreasing the peak current and the electrochemical activity. These results are consistent with the cycling performance results observed in Fig. 3. The  $\text{LiMg}_{0.02}\text{Mn}_{1.98}\text{O}_4$  electrode prepared for calcination time of 6 h reveals higher anodic and cathodic peak currents, indicating the lower internal

resistance and better electrochemical reactivity [14], the result were consistent with the previous cycling performance analysis.

#### 4. CONCLUSIONS

Single phase  $\text{LiMg}_{0.02}\text{Mn}_{1.98}\text{O}_4$  cathode materials with a good crystallinity were synthesized at 500 °C for calcining various time by a solid-state combustion synthesis. The initial specific discharge capacity of  $\text{LiMg}_{0.02}\text{Mn}_{1.98}\text{O}_4$  can be enhanced by extending calcination time. The cycling performance of  $\text{LiMg}_{0.02}\text{Mn}_{1.98}\text{O}_4$  materials were improved ascribe to Mg-doping. Specifically,  $\text{LiMg}_{0.02}\text{Mn}_{1.98}\text{O}_4$  synthesized for calcination time of 6 h reveals the excellent electrochemical performance with an initial specific discharge capacity of 107.2 mAh g<sup>-1</sup> at 0.2 C and a capacity retention of 88.62% after 100 cycles.

#### ACKNOWLEDGEMENTS

This work was financially supported by the National Natural Science Foundation of China (51062018, 51262031, 51362012), the Natural Science Foundation of Yunnan (2010FXW004, 2012FB173), Program for Innovative Research Team (in Science and Technology) in University of Yunnan Province (2010UY08, 2011UY09), and Yunnan Provincial Innovation Team (2011HC008).

#### References

1. X. L. Li, R. M. Xiang, T. Su and Y. T. Qian, *Mater. Lett.*, 61 (2007) 3597.
2. T. F. Yi, L. C. Yin, Y. Q. Ma, H. Y. Shen, Y. R. Zhu and R. S. Zhu, *Ceram. Int.*, 39 (2013) 4673.
3. B. Xu, D. N. Qian, Z. Y. Wang and Y. S. Meng, *Mater. Sci. Eng. R*, 73 (2012) 51.
4. B. L. He, W. J. Zhou, Y. Y. Liang, S. J. Bao and H. L. Li, *J. Colloid Interface Sci.*, 300 (2006) 633.
5. X. Y. Feng, C. Shen, X. Fang and C. H. Chen, *J. Alloys Compd.*, 509 (2011) 3623.
6. J. H. Lee, J. C. Lee, M. K. Park and S. Park, *J. Mater. Process. Tech.*, 171 (2006) 240.
7. M. Kotobuki, Y. Isshiki, H. Munakata and K. Kanamura, *Electrochim. Acta*, 55 (2010) 6892.
8. S. J. Shi, J. P. Tu, Y. Y. Tang, X. Y. Liu, X. Y. Zhao, X. L. Wang and C. D. Gu, *J. Power Sources*, 241 (2013) 186.
9. M. Helan, L. John Berchmans, T. P. Jose, A. Visuvasam and S. Angappan, *Mater. Chem. Phys.*, 124 (2010) 439.
10. D. Arumugam, G. Paruthimal Kalaignan and P. Manisankar, *Solid State Ionics*, 179 (2008) 580.
11. W. M. Xu, A. B. Yuan, L. Tian and Y. Q. Wang, *J. Appl. Electrochem.*, 41 (2011) 453.
12. H. M. Wu, J. P. Tu, Y. F. Yuan, X. T. Chen, J. Y. Xiang, X. B. Zhao and G. S. Cao, *J. Power Sources*, 161 (2006) 1260.
13. X. Y. Zhou, M. M. Chen, C. W. Su, Y. Xia, X. Z. Huang, Y. J. Zhang and J. M. Guo, *Adv. Mater. Res.*, 353 (2012) 581.
14. X. Y. Zhou, M. M. Chen, M. W. Xiang, H. L. Bai and J. M. Guo, *Ceram. Int.*, 39 (2013) 4783.
15. L. F. Xiao, Y. Q. Zhao, Y. Y. Yang, X. P. Ai, H. X. Yang and Y. L. Cao, *J. Solid State Electrochem.*, 12 (2008) 687.
16. H. M. Wu, J. P. Tu, Y. F. Yuan, Y. Li, W. K. Zhang and H. Huang, *Physica. B*, 369 (2005) 221.
17. J. W. Lee, J. I. Kim, K. C. Roh, S. M. Par and K. Kim, *Solid State Sci.*, 12 (2010) 1687.
18. P. Singh, A. Sil, M. Nath and S. Ray, *Ceram. Silik.*, 54 (2010) 38.
19. P. Strobel, A. Ibarra Palos, M. Anne and F. Le Cras, *J. Mater. Chem.*, 10 (2000) 429.
20. G. M. Song, W. J. Li and Y. Zhou, *Mater. Chem. Phys.*, 87 (2004) 162.

21. J. L. Wang, Z. H. Li, J. Yang, J. J. Tang, J. J. Yu, W. B. Nie, G. T. Lei and Q. Z. Xiao, *Electrochim. Acta*, 75 (2012) 115.
22. Z. L. Liu, A. S. Yu and J.Y. Lee, *J. Power Sources*, 74 (1998) 228.
23. M. Prabu, M. V. Reddy, S. Selvasekarapandian, G. V. Subba Rao and B. V. R. Chowdari, *Electrochim. Acta*, 88 (2013) 745.
24. M. X. Tang, A. B. Yuan, H. B. Zhao, J. Q. Xu, *J. Power Sources*, 235 (2013) 5.

© 2014 by ESG ([www.electrochemsci.org](http://www.electrochemsci.org))